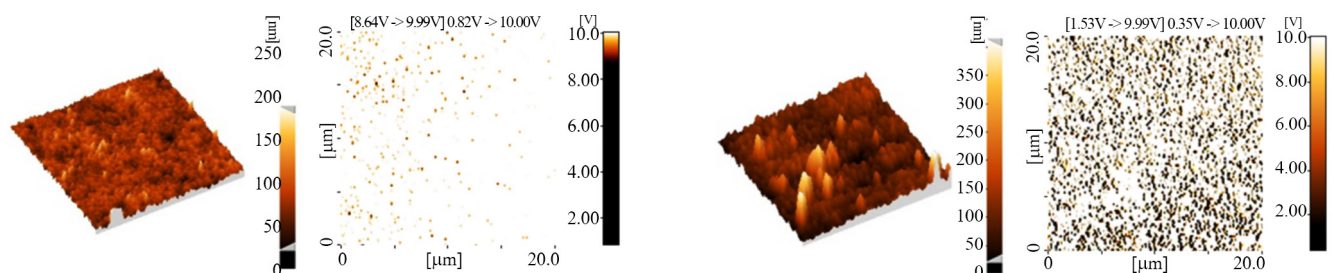


**Figure 3.** Increasing zeta potential of synthesized film containing 10% AA from  $G_0$  to  $G_4$ .

beyond the first generation, only the terminal carboxylic groups at the periphery are accessible which confirms the formation of dense shell dendritic structure owing to the increased steric hindrance [15, 19]. Besides, the reduction in conversion with increasing generation is a major obstacle in the way of increasing the number of end functional groups [11].

Since wettability can be governed by surface roughness, the topography of the synthesized films containing 10% AA for  $G_0$  and  $G_4$  was studied by AFM as shown in Figure 4 and the calculated roughness is tabulated in Table 2. As can be seen, there is an increase in the roughness with successive generation from 13 nm in  $G_0$  up to 31 nm in  $G_4$ , validating the obtained results of contact angle measurements. In other words, the hydrophilicity of dendrigraft structures declines with increasing step number due to the restricted mobility or steric hindrance of terminal groups. Zhang et al. [42] showed that with increasing surface roughness, the fraction of air trapped at the interface between solid surface and water increases obviously, which results in higher contact angle. Based on Wenzel modified Young's equation, contact angle  $\theta'$  on a rough surface can be determined by the following equation:

$$\cos \theta' = \gamma \frac{(\gamma_{SV} - \gamma_{SL})}{\gamma_{LV}} = \gamma \cos \theta \quad (6)$$



**Figure 4.** AFM image of P(AN/AA)film containing 10% AA: (a)  $G_0$  and (b)  $G_4$ .

**Table 2.** Mean roughness of P(AN/AA)film containing 10% AA from  $G_0$  to  $G_4$ .

| Sample    | Average roughness (nm) |
|-----------|------------------------|
| <b>G0</b> | 13                     |
| <b>G1</b> | 15                     |
| <b>G2</b> | 20                     |
| <b>G3</b> | 27                     |
| <b>G4</b> | 31                     |

where  $r$  is the roughness factor, defined as the ratio of the actual area of a rough surface to the geometric projected area,  $\gamma_{SV}$ ,  $\gamma_{SL}$  and  $\gamma_{LV}$ , respectively, denote the interfacial free energies per unit area of the solid-gas, solid-liquid, and liquid-gas interfaces [43]. In the regime of Wenzel's equation, the surface free energy of the solid part of a rough surface is  $r$  times higher than that of a flat surface and the hydrophobicity of a rough hydrophobic surface is augmented by the increase of the solid-liquid contact area. Therefore, the contact angle and its hysteresis (the difference between advancing and receding contact angles) on hydrophobic rough surfaces increase as the roughness factor increases [44]. It seems that another important factor which affects the hydrophilicity of the P(AN/AA) dendrigrated with CA is related to the increasing roughness of the film by increasing step numbers.

## CONCLUSIONS

The hydrophilic properties of P(AN/AA) film with 5, 10 and 20% of acrylic acid were evaluated after the formation of citric acid dendrigrated in a heterogeneous system. The FTIR spectra confirmed the formation of intermolecular hydrogen bonding after dendrigraft formation, affecting the wettability of the films. The cleavage of hydrogen bonding after reaction with  $\text{NaHCO}_3$  was also observed. The results of contact angle measurement showed a decline in contact



21. Akbari S, Kish MH, Entezami AA (2010) Modification of acrylonitrile/acrylic acid copolymer films and fibers by dendrigrift formation. *Polym Int* 59: 1550-1557
22. Abdouss M, Mousavi Shoushtari A, Majidi Simakani A, Akbari S, Haji A (2014) Citric acid-modified acrylic micro and nanofibers for removal of heavy metal ions from aqueous media. *Desalin Water Treat* 52: 7133-7142
23. Akbari S (2016) Thermal analysis of acrylonitrile/acrylic acid copolymer dendrigrated with citric acid. *J Text Polym* 4: 27-36
24. Chami Khazraji A, Robert S (2013) Self-assembly and intermolecular forces when cellulose and water interact using molecular modeling. *J Nanomater* 2013: 10.1155/2013/745979
25. Miwa M, Nakajima A, Fujishima A, Hashimoto K, Watanabe T (2000) Effects of the surface roughness on sliding angles of water droplets on superhydrophobic surfaces. *Langmuir* 16: 5754-5760
26. Fürstner R, Barthlott W, Neinhuis C, Walzel P (2005) Wetting and self-cleaning properties of artificial superhydrophobic surfaces. *Langmuir* 21: 956-961
27. Li S, Huang J, Ge M, Cao C, Deng S, Zhang S, Chen G, Zhang K, Al-Deyab SS, Lai Y (2015) Self-cleaning cotton: Robust flower-like TiO<sub>2</sub>@cotton fabrics with special wettability for effective self-cleaning and versatile oil/water separation (*Adv. Mater. Interfaces* 14/2015). *Adv Mater Interfaces* 2: 10.1002/admi.201570068
28. Sadeghi P, Tavanai H, Khoddami A (2017) Hydrophobicity of fluorocarbon-finished electrospun poly (acrylonitrile) nanofibrous webs. *J Text Inst* 108: 189-195
29. Zhang M, Feng S, Wang L, Zheng Y Lotus effect in wetting and self-cleaning. *Biotribology* 5: 31-43
30. Yuan Y, Lee TR (2013) Contact angle and wetting properties. In: *Surface science techniques*. Bracco G, Holst B (Eds), Springer, 3-34
31. Kubiak K, Wilson M, Mathia T, Carval P (2011) Wettability versus roughness of engineering surfaces. *Wear* 271: 523-528
32. Krumpfer JW, McCarthy TJ (2010) Contact angle hysteresis: A different view and a trivial recipe for low hysteresis hydrophobic surfaces. *Faraday Discuss* 146: 103-111
33. Gao L, McCarthy TJ (2006) Contact angle hysteresis explained. *Langmuir* 22: 6234-6237
34. Xu QF, Liu Y, Lin F-J, Mondal B, Lyons AM (2013) Superhydrophobic TiO<sub>2</sub>-polymer nanocomposite surface with UV-induced reversible wettability and self-cleaning properties. *ACS Appl Mater Interfac* 5: 8915-8924
35. Pawlak Z, Urbaniak W, Oloyede A (2011) The relationship between friction and wettability in aqueous environment. *Wear* 271: 1745-1749
36. Bajaj P, Paliwal D, Gupta A (1993) Acrylonitrile-acrylic acids copolymers. I. Synthesis and characterization. *J Appl Polym Sci* 49: 823-833
37. Wu J, Lin J, Li G, Wei C (2001) Influence of the COOH and COONa groups and crosslink density of poly(acrylic acid)/montmorillonite superabsorbent composite on water absorbency. *Polym Int* 50: 1050-1053
38. Yang CQ (1991) Characterizing ester crosslinkages in cotton cellulose with FT-IR photoacoustic spectroscopy 1. *Text Res J* 61: 298-305
39. Janorkar AV, Luo N, Hirt DE (2004) Surface modification of an ethylene-acrylic acid copolymer film: Grafting amine-terminated linear and branched architectures. *Langmuir* 20: 7151-7158
40. Walters KB, Hirt DE (2007) Synthesis and characterization of a tertiary amine polymer series from surface-grafted poly (tert-butyl acrylate) via diamine reactions. *Macromolecules* 40: 4829-4838
41. de Gennes P-G, Hervet H (1983) Statistics of "starburst" polymers. *J Phys Let* 44: 351-360
42. Zhang J, Han Y (2008) A topography/chemical composition gradient polystyrene surface: Toward the investigation of the relationship between surface wettability and surface structure and chemical composition. *Langmuir* 24: 796-801
43. Wenzel RN (1949) Surface roughness and contact angle. *J Phys Chem* 53: 1466-1467
44. Tsai P-S, Yang Y-M, Lee Y-L (2006) Fabrication of hydrophobic surfaces by coupling of Langmuir-Blodgett deposition and a self-assembled monolayer. *Langmuir* 22: 5660-5665